

AD 682552

Massachusetts Institute of Technology
Cambridge, Massachusetts 02139

TITLE

Application of Gas Lasers to Studies of Fundamental Molecular
and Atomic Processes

Annual Technical Report #1

for combined periods: January 1, 1968 to June 30, 1968
and July 1, 1968 to December 31, 1968

Under Supervision of

Principal Investigator: Professor Ali Javan
617 - 864-6900 x5088

Under

Contract # N00014-67-A-0204-0014
Program Code # 8E30

FEB 25 1969

has been approved
and sale; its
dated

Sponsored By

Advanced Research Projects Agency
ARPA Order No. 306

Contract Starting Date: July 1, 1967
Contract Termination Date: June 30, 1969
Contract Total: \$100,000-
M. I. T. Project Number: DSR 70620

Issue Date: January 20, 1969

This report consists of a summary and several appendices.

SUMMARY

Measurements related to important aspects of molecular energy transfer and vibrational relaxation in CO_2 are continuing. Pressure dependence of the imprisoned radiative decay rate of the 001 level arising from the 4.35μ photon reabsorption in 001 \rightarrow 000 transitions is established in detail. A detailed study of the coupling of 001 state with other nearby vibrational states is also underway.

Measurements of the motional narrowing of the line profile of the spontaneous vibrational Raman scattering in H_2 are completed. The motional narrowing effect is observed in considerable detail. The results show unambiguously that of the two existing theories, the one based on a hard collision model is in better agreement with observation as compared to the one based on soft collision model.

Propagation of short pulses through a resonantly absorbing medium is being studied both theoretical and experimentally. In this connection, boundary reflection resulting from signal velocity reduction in self-induced transparency is theoretically analyzed and estimated. The transparency behavior is shown to merge into the linear dispersion behavior away from the resonance. The use of the pulse delays as a qualitative indicator of transparency is analyzed in detail. There exist numerous transitions which do not satisfy criterion for existence of self-induced transparency. In these systems, however, the absorption coefficient for a narrow pulse is appreciably below that of a wide pulse. These considerations which are based on

a recent detailed theoretical analysis are being studied experimentally in gaseous systems. In this connection, transmission behavior of 10.6μ CO_2 laser radiation pulse is examined in gaseous SF_6 at varying pressures. It is shown that, contrary to a previous report, the observed behavior may be explained on the basis of non-linear population saturation without any coherent effect associated to self-induced transparency. Furthermore, new pulse reshaping features are observed in SF_6 and explained theoretically. (These results are currently being prepared for publication.)

Experiments on laser-induced line narrowing effect is being pursued. Also, exploration of gas laser transitions within levels having a broad atomic velocity distribution in the upper laser level and a narrow velocity distribution in the lower level is in progress.

Short Pulse Transmission Experiments in SF₆
C. K. Rhodes, A. Szöke, and A. Javan

In a recent theoretical investigation, ⁽¹⁾ we have analyzed several aspects of propagation behavior of a short radiation pulse through an absorbing medium. This analysis shows that a number of important propagation effects are highly dependent on the angular momentum quantum numbers of the transition responsible for absorption in the medium. It is shown, for instance, that an absorbing medium consisting of a $J \rightarrow J + 1$ transition with $J > 0$, cannot sustain a short pulse propagation with a self-induced transparency characteristic corresponding to an undistorted and unattenuated pulse propagation; a $J = 0 \rightarrow 1$ transition, on the other hand, is capable of sustaining complete self-induced transparency. Further theoretical analysis (which includes the effect of inhomogeneous broadening) shows that short pulse attenuation factor for $J \rightarrow J + 1$ with $J > 0$ is a sensitive function of the pulse shape; in fact for an appropriate pulse shape, the attenuation factor may be considerably reduced below that expected normally for an arbitrarily long pulse saturating the absorbing transition.

In an earlier publication by Patel and Slasher, ⁽²⁾ it was reported that gaseous SF₆ provides an unidentified absorption resonance at one of the P-branch transitions at 10.6 μ which shows a self-induced transparency effect similar to the one observed earlier by Hahn and McCall in ruby. We find, however, that the absorption in SF₆ is of the type that can not admit complete self-induced transparency. On the other hand, the SF₆ resonance provides an excellent means of studying

important questions regarding transmission of a short pulse.

This report will sketch our current activity on the examination of short pulse propagation in SF_6 . Preliminary findings indicate that experimental results⁽²⁾ may be explained on the basis of an effective non-linear population saturation effect which has a tendency to mask an coherent effect. This view has support on several sides. They are the following:

- a) Pulse transmission experiments which indicate an effective population saturation effect.
- b) Theoretical considerations concerning the effect of level degeneracy which modifies the characteristic pulse shape. ()
- c) Spectroscopic evidence that the observed absorption in SF_6 is not due to a single resolved level in the 10.6μ band.

These points will be examined in the text below.

The theory of self-induced transparency predicts that, for a given absorber characterized by T_2 , the behavior of the transmitted intensity versus the input intensity should differ for pulses described by $\tau_{\text{pulse}} < T_2$ as opposed to the opposite case $\tau_{\text{pulse}} > T_2$. A pulse transmission experiment has been done which gave the following results. The input pulse is shown in Fig. 1; the output intensity versus input intensity curve is illustrated in Fig. 2. For our purposes, the single pulse can be considered as a pair

of pulses each satisfying the conditions stated above. In the presence of the coherent self-induced transparency effect one would expect an enhanced transmission of the peak (A) as compared to the tail (B). However, the data in Fig. 2 show a result which is contrary to this conclusion; the peak and the tail are transmitted similarly. In addition, no significant pulse reshaping was observed. It is important to note that Fig. 2 clearly shows a non-linear region for both the peak (A) and the tail (B).

Another series of pulse transmission experiments which gave complementary information has been performed. In this experiment short (~ 300 nsec width) Q-switched pulses were passed through an SF₆ absorption cell whose pressure was continuously lowered. Figure 3 shows a photograph which consists of a sequence of exposures taken at successively lower SF₆ pressures in the absorption cell. The photograph clearly shows that the transmitted pulse is significantly sharpened on its leading edge at an intermediate SF₆ pressure. This behavior is seen on the P(16) line of CO₂ and not on any of the other nearby lines (e. g. P(18) or P(20)).

The influence of several degenerate levels in relation to these observations is being examined. A machine calculation indicates the following results.

1. A number of degenerate levels smears the knee in the output intensity vs input intensity curves.
2. Delay times are generally reduced as compared to the situation involving only a single non-degenerate transition.

3. For high input intensities (i. e. $\mu \int_{-\infty}^{\infty} \mathcal{E}(t) dt \gg \pi$) a pulse steepening effect appears similar to that observed in Fig. 3.

Finally, the suspicion that the absorption of the P(16) line of CO_2 by SF_6 is not due to a single resolved, Doppler broadened transition has been confirmed experimentally. The absorption has been measured as a function of pressure from 5μ SF_6 pressure to 17mm SF_6 pressure. The absorption rises linearly with pressure all the way to 17mm of SF_6 . This indicates that the resonance is not a single, resolved transition since 17mm is well above any reasonable limit for pressure broadening at 10.6μ .

All these results indicate that the coherent self-induced transparency effect is considerably modified and complicated by level degeneracy and overlapping transitions.

REFERENCES

1. C. K Rhodes, A. Szöke and A. Javan, Phys. Rev. Letters 21, 1151 (1968).
2. C. K. N. Patel and R. E. Slusher, Phys. Rev. Letters 19, 1019 (1967).

FIGURE CAPTIONS

1. Input Pulse Shape
2. Output Intensity vs. Input Intensity at $17.1 \mu \text{SF}_6$.
3. Pulse Steepening on P(16) as SF_6 Pressure is Lowered.

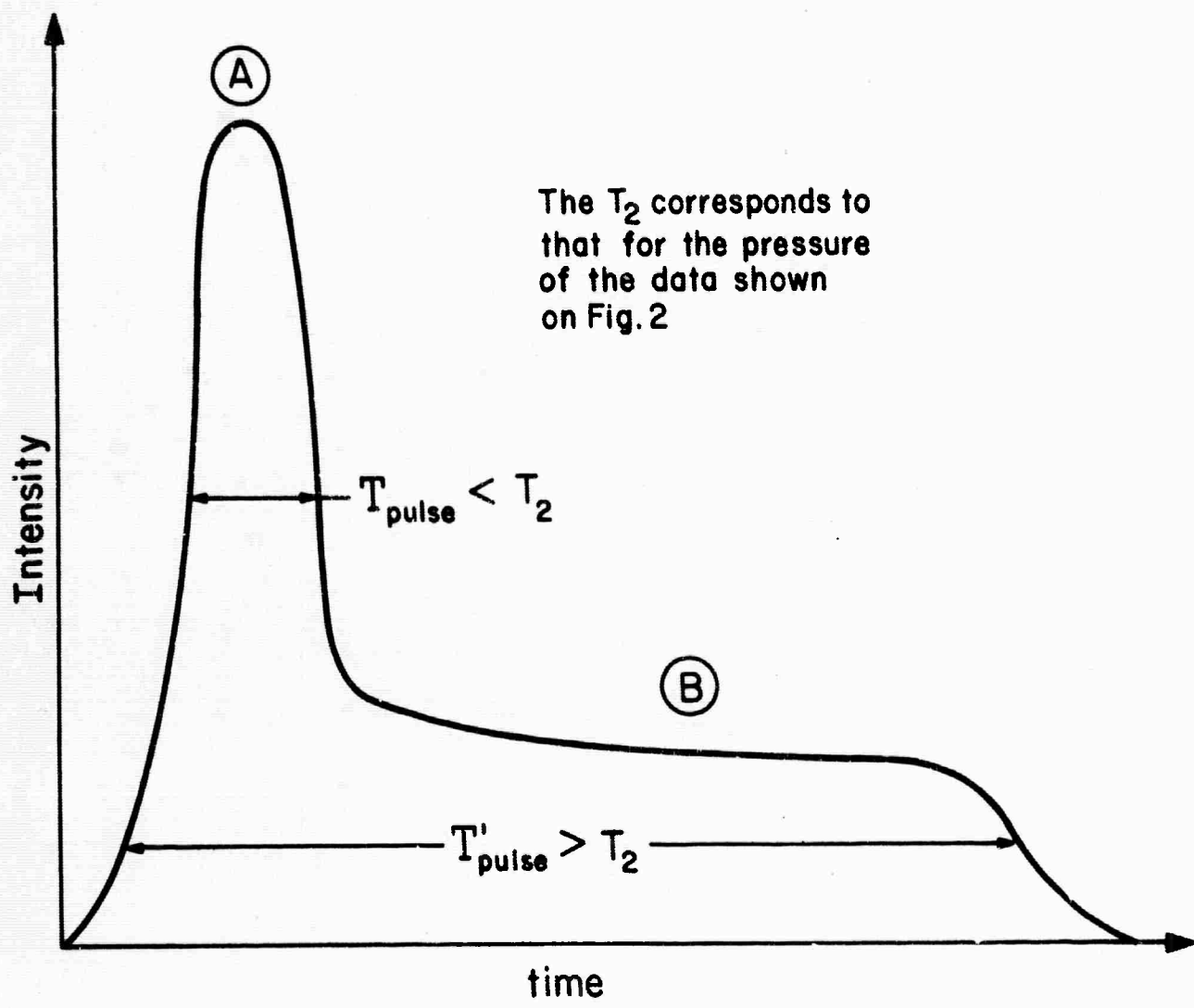


FIGURE 1

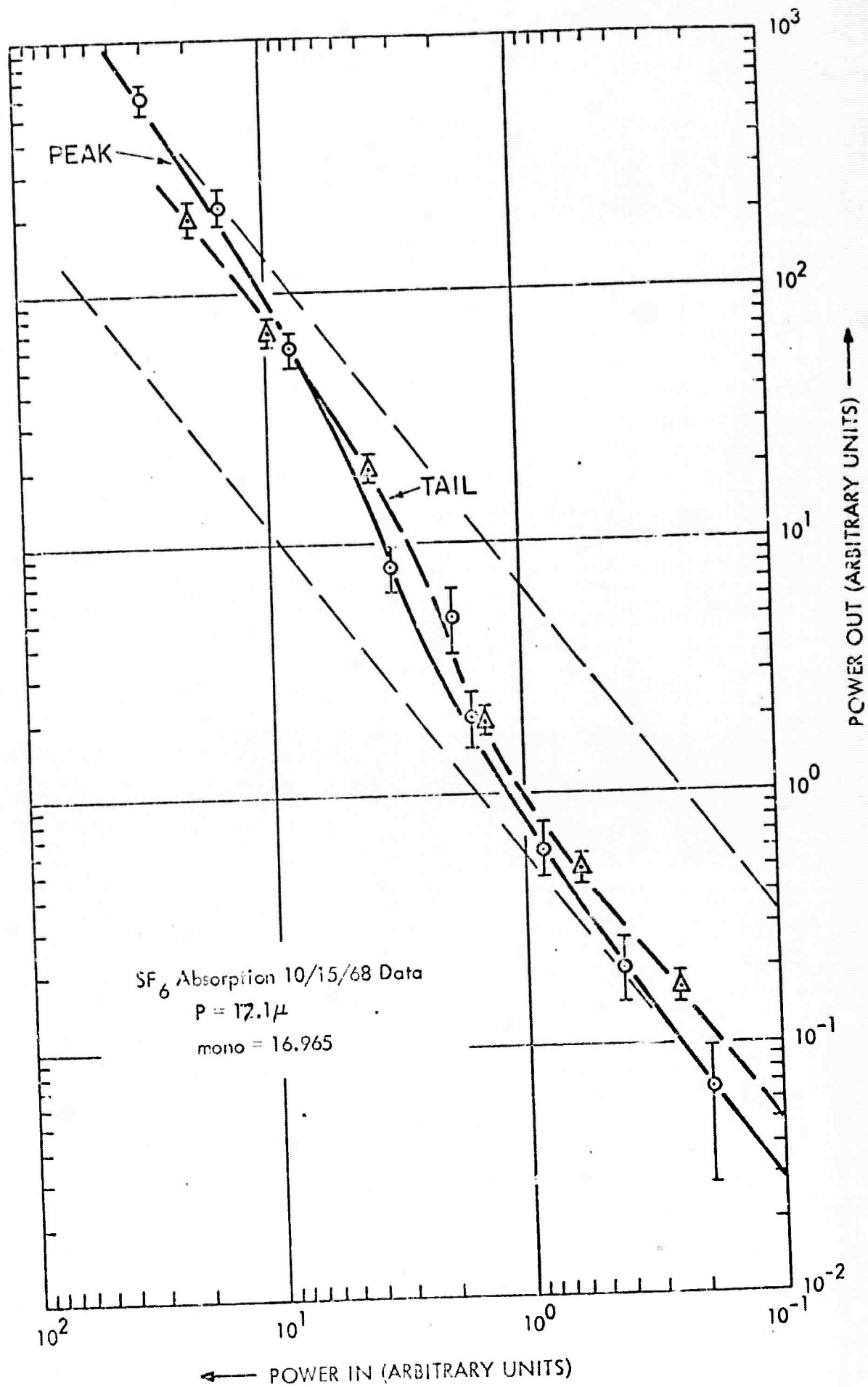


FIGURE 2

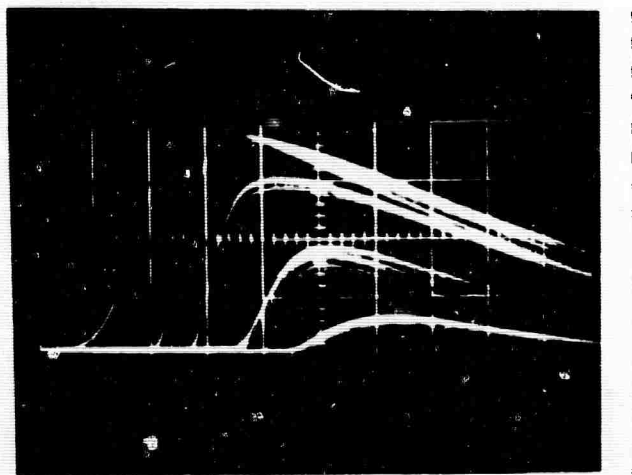


FIGURE 3

ON CONSEQUENCES OF THE DIFFERENT PHASE AND SIGNAL
VELOCITIES IN SELF-INDUCED TRANSPARENCY

A. Szoke

Boundary reflection resulting from signal velocity reduction in self-induced transparency is estimated. The transparency behavior is shown to merge into the linear dispersion behavior away from resonance. Conclusions are drawn about using pulse delays as qualitative indicators of transparency.

* * * * *

Self-Induced transparency is a phenomenon whereby optical pulses propagate in a resonant medium without absorption or distortion. The effect is accompanied by a large reduction of the pulse envelope propagation velocity [1], whereas the phase velocity is unaffected if the optical carrier is exactly on resonance. It seemed of interest to consider the consequences this effect has on the EM wave and, in particular, to estimate the reflection of a pulse at the boundaries of the resonant medium.

For a simple two-level system, inhomogeneously broadened, assuming circular polarization of the EM wave, the electric vector as given by McCall and Hahn [2] is:

$$\vec{E}(z, t) = \frac{1}{p\tau} \operatorname{sech} \left[\frac{1}{\tau} \left(t - \frac{z}{V} \right) \right] \operatorname{Re} \{ (\vec{x} + iy) e^{i(\omega t - k'z)} \} . \quad (1)$$

The envelope propagation velocity is given by:

$$\frac{1}{V} = \frac{\eta}{c} + A \tau^2 \int \frac{g(\Omega) d\Omega}{1 + (\Delta\omega\tau)^2} \quad (2)$$

and the propagation vector is:

$$k' = k + A\tau \int \frac{(\Delta\omega\tau) g(\Omega) d\Omega}{1 + (\Delta\omega\tau)^2} \quad (3)$$

with $A = 4\pi N\omega p^2 / \eta c \hbar$. The normalized spectral distribution function of the atomic resonance frequencies Ω , centered at Ω_0 , is $g(\Omega)$, and $\Delta\omega = \Omega - \omega$. The free parameter τ fixes the pulse duration, p is the transition matrix element, $k = \eta\omega/c$ is the propagation vector of the optical carrier in the host medium of refractive index η , and N is the density of resonant systems. The magnetic vector \vec{H} of the EM wave is obtained from eq. (1) using $\vec{\nabla} \times \vec{E} = -1/c \partial \vec{H} / \partial t$, and to order $1/\omega\tau$ is given by:

$$\begin{aligned} \vec{H}(z, t) = & \frac{\eta'}{p\tau} \operatorname{sech} \left[\frac{1}{\tau} \left(t - \frac{z}{V} \right) \right] \operatorname{Re} \{ \hat{y} - i\hat{x} \} e^{i(\omega t - k'z)} \\ & + \left(\frac{c}{V} - \eta \right) \frac{1}{\omega p \tau^2} \operatorname{sech} \left[\frac{1}{\tau} \left(t - \frac{z}{V} \right) \right] \tanh \left[\frac{1}{\tau} \left(t - \frac{z}{V} \right) \right] \operatorname{Re} \{ (\hat{x} + i\hat{y}) e^{i(\omega t - k'z)} \} \end{aligned} \quad (4)$$

where $\eta' = k'c/\omega$. This result can be obtained either by Fourier analysis of the \vec{E} field or by direct integration. The second term in \vec{H} is an anomalous component which is caused by the difference between signal and phase velocities, and which is 90° out of phase with the usual component of \vec{H} .

The boundary reflection can be calculated conveniently for an incident wave whose behavior is known in the material, using the boundary conditions on \vec{E} and \vec{H} . The \vec{E} field of a normally incident wave giving an exact 2π -pulse (eqs. (1), (4)) inside the medium is found to be, at the boundary ($z = 0$):

$$\begin{aligned} \vec{E}_{\text{ext}} = & \frac{1}{p\tau} \operatorname{Re} \left\{ \left[\frac{1 + \eta'}{2} \operatorname{sech} \left(\frac{t}{\tau} \right) \right. \right. \\ & \left. \left. + \frac{i}{2} \left(\frac{c}{V} - \eta' \right) \frac{1}{\omega\tau} \operatorname{sech} \left(\frac{t}{\tau} \right) \tanh \left(\frac{t}{\tau} \right) \right] (\hat{x} + i\hat{y}) e^{i\omega t} \right\} . \end{aligned} \quad (5)$$

The first term corresponds to Fresnel reflection with refractive index η' ; the dispersion due to the two-level system, eq. 3, is included in η' . The second term is the phase-shifted anomalous component, proportional to the derivative of the pulse envelope and to the velocity reduction. A similar term is obtained in linear dispersion theory, as a consequence of the linearity of Maxwell's equation $\nabla \times \vec{E} = -1/c \partial \vec{H} / \partial t$. The reflection at the exit of the resonant medium is of similar strength. These results, obtained in the slowly varying envelope approximation, are expected to hold qualitatively in an exact theory.

It is interesting to point out that the self-induced transparency results merge into those of linear dispersion theory in the limit where the optical carrier frequency ω is displaced far away from the resonance frequency Ω_0 . In that limit, eqs. (2) and (3) reduce to $1/V = \eta/c + A/(\Omega_0 - \omega)^2$ and $k' = k + A/(\Omega_0 - \omega)$. These are identical to the results of linear dispersion theory [3]; in particular, one sees that the signal velocity merges into the group velocity given by $V^{-1} = \partial k' / \partial \omega$. Similarly, eq. (1) describes properly, except for a constant coefficient, the propagation of a pulse in small signal theory, provided absorption caused by homogeneous broadening $\Gamma = 1/T_2'$ can be neglected. Finally, eqs. (4) and (5) give then the proper H field and boundary reflection.

Let us now consider the time evolution of a pulse in a retarded reference frame ($t - \eta z/c$). In a medium of length ΔL , the relative decrease of the small signal envelope amplitude is $\Delta E/E = \alpha \Delta L/2$, where α is the absorption constant, and the fractional small signal pulse delay is $\Delta t/\tau = (1/V - \eta/c)\Delta L/\tau$. When the ratio of these quantities is larger than unity, $(\Delta E/E)/(\Delta t/\tau) > 1$, the pulse is attenuated more than it is delayed and it always remains under the initial pulse envelope in the retarded reference frame. When this ratio is smaller than unity, the peak of the pulse moves beyond the input pulse tail, as it propagates

through the medium. Far from resonance the small signal absorption constant is given by $\alpha = 2\Gamma A / (\Omega_0 - \omega)^2$, proportional to the velocity reduction as given above. One finds then $(\Delta E/E) / (\Delta t/\tau) = \Gamma \tau$. But the condition $\Gamma \tau = \tau/T_2' < 1$ is precisely that which is required to obtain transparency. Therefore the qualitative observation of a pulse delay beyond the input pulse tail is not sufficient evidence of transparency. When $\Gamma \tau < 1$, any pulse in the wings of the resonance line would exhibit a delay which becomes appreciable when the carrier frequency is moved closer to resonance. Obviously these simple arguments do not apply on resonance, where the small signal envelope velocity is ill-defined [4] and small signal theory must deal with particular pulse shapes and inhomogeneous broadening. This work was done in collaboration with E. Courtens, IBM Zurich Research Laboratory, 8803 Rüschlikon-ZH, Switzerland.

REFERENCES

1. Impulseinhüllendenfortpflanzungsgeschwindigkeit.
2. S. L. McCall and E. L. Hahn, Phys. Rev. Letters 18, 908 (1967).
3. Leon Brillouin, Wave Propagation and Group Velocity, Academic Press 1960.
4. Ibid. pp. 121 to 124.

Motional Narrowing in Hydrogen Raman Scattering

J. R. Murray and A. Javan

This report describes the results of a high resolution study of the motional narrowing effect (the decrease in the normal Doppler linewidth when the mean free path becomes comparable to the wavelength of the emitted radiation (1 - 5)) in spontaneous Raman scattering in the $\alpha(1)$ line of the 1-0 vibrational band of the hydrogen molecule. An argon ion laser is used as the exciting source, and the linewidth analysis is done with a Fabry-Perot interferometer.

We have reported qualitative preliminary observations of this effect previously (6). Motional narrowing was first seen in hydrogen by Rank and Wiggins in infrared absorption spectra (7). Narrowing has also been seen in stimulated Raman scattering in hydrogen (8). Cooper, May, et al. have obtained similar high resolution results for the rotational Raman lines of hydrogen. (9)

The argon ion laser operates at 4880\AA and is a hollow cathode design with segmented graphite discharge tube (10). The laser is operated in a four mirror Michelson type cavity (11) to reduce the number of simultaneously oscillating modes, and has a linewidth of about 0.0085 cm^{-1} . (The linewidth under similar conditions in a two mirror cavity is about 0.1 cm^{-1} .) The center of this line is locked to an external Fabry-Perot reference to reduce frequency drifts, which otherwise are a severe limitation. The output power is about 50 milliwatts.

The laser beam enters a scattering cell which is a quartz capillary of 0.5 mm. inner diameter and 30 cm length. Reflection at grazing incidence from the walls of this capillary propagates the light scattered in

a small cone in the forward (parallel to the laser beam) and backward (anti-parallel) directions to the ends of the cell, where it is collimated by a lens and enters a pressure scanned Fabry-Perot interferometer of 0.79 cm^{-1} interorder spacing. The output of the Fabry-Perot is detected by an ITT FW-130 photomultiplier with pulse counting electronics and displayed on a chart recorder. Recordings are made at a temperature of 25°C . over a density range of 2 to 100 A magat. Sample recordings exhibiting the line narrowing effect are shown in Figure 1. The dependence of the Q(1) linewidth on density is shown in Figure 2. The instrumental linewidth (0.031 cm^{-1}) has been subtracted from each point.¹

At high densities, ignoring pressure broadening effects, all models of the motional narrowing predict that the normal Gaussian Doppler profile will become a Lorentzian lineshape with full width at half maximum $\frac{D_0 k^2}{\pi d}$, where D_0 is the self-diffusion constant, k is the wave vector of the incident photon minus the wave vector of the emitted photon, and d is the density in A magat units (density/density at 1 atm. pressure and 0°C). If pressure broadening is present and is not correlated with the motional narrowing (2-5), the resulting lineshape will be a Lorentzian of width $\frac{D_0 k^2}{\pi d} + ad$, where a is the pressure broadening coefficient, and is determined from the forward scattering data to be $1.68 \pm .07 \times 10^{-3} \text{ cm}^{-1}/\text{A magat}$, which is in fair agreement with the calculations of Van Kranendonk (12) and the measurement at higher densities by May, et al. (13).

The solid line for the backward scattering in Figure 2 gives a fit to this simple diffusion model. The dotted line gives the behavior of a "hard collision" model (3, 4) in the region where it diverges from the simple diffusion model. This model assumed that the velocity of a molecule after a collision

has a Maxwell-Boltzmann distribution and is unrelated to its velocity before the collision. The diffusion constant D_0 has been chosen for a best fit to this model, and is $1.35 \pm .10 \text{ cm}^2 \text{ Amagat/sec}$. A gas kinetic measurement of D_0 (14), expressed in our units, and corrected for temperature, gives $D_0 = 1.361 \pm .004 \text{ cm}^2 \text{ Amagat/sec}$. As a measure of fit of the experimental data to these models, the mean deviation of the experimental points from the simple diffusion model above 12 Amagat is (all in units of 10^{-3} cm^{-1}) $+0.9$ and the root mean square deviation is ± 3 . For the hard collision model below 12 Amagat the mean deviation is $+0.07$ and the rms deviation ± 7.5 . Noise in the points above 12 Amagat is primarily laser flicker. Statistical noise is important below 12 Amagat.

The dashed line gives the behavior of a Brownian motion or "soft collision" model (2, 4) for the same region and with the same value of D_0 . This model assumes a small velocity change in a single collision. If D_0 is chosen 10% lower for a best fit to the Brownian motion model, the mean deviation below 12 Amagat is -5 and the rms deviation ± 10 . Above 12 Amagat the mean deviation is $+3$ and the rms deviation is ± 4 . This is a noticeably worse fit than for the hard collision model, and indicates that the hard collision model is a better approximation for hydrogen.

We are presently extending these measurements to other lines in hydrogen and deuterium.

We would like to acknowledge very helpful discussions with Professor A. D. May.

REFERENCES

1. R. H. Dicke, Phys. Rev. 89, 472 (1953).
2. L. Galatry, Phys Rev. 122, 1218 (1961).
3. M. Nelkin and A. Ghatak, Phys. Rev. 135, A4 (1964).
4. S. G. Rautian and I. I. Sobelmann, Usp. Fiz. Nauk. 90, 209 (1966).
5. J. I. Gersten and H. M. Foley, J. Opt. Soc. Am. 58, 933 (1968).
6. J. Murray and A. Javan. Bull. Am. Phys. Soc. 12, 113 (1967).
7. D. H. Rank and T. A. Wiggins, J. Chem. Phys. 39, 1348 (1963).
8. P. Lallemand, P. Simova, and G. Bret, Phys. Rev. Lett, 17, 1239 (1966).
9. V. G. Cooper, A. D. May, E. H. Hara, and H. F. P. Knapp, Can. J. Phys. 46, 2019 (1968).
10. D. A. Huchital and J. D. Rigden, IEEE J. Quant. Elect. 3, 378 (1967).
11. P. W. Smith, IEEE J. Quant. Elect. 1, 343 (1965).
12. J. Van Kranendonk, Can. J. Phys. 41, 433 (1963).
13. A. D. May, V. Degen, J. C. Stryland, and H. L. Welsh, Can. J. Phys. 39, 1769 (1961).
14. P. Harteck and H. W. Schmidt, Z. Physik. Chem., Abt. B, 21, 447 (1933).

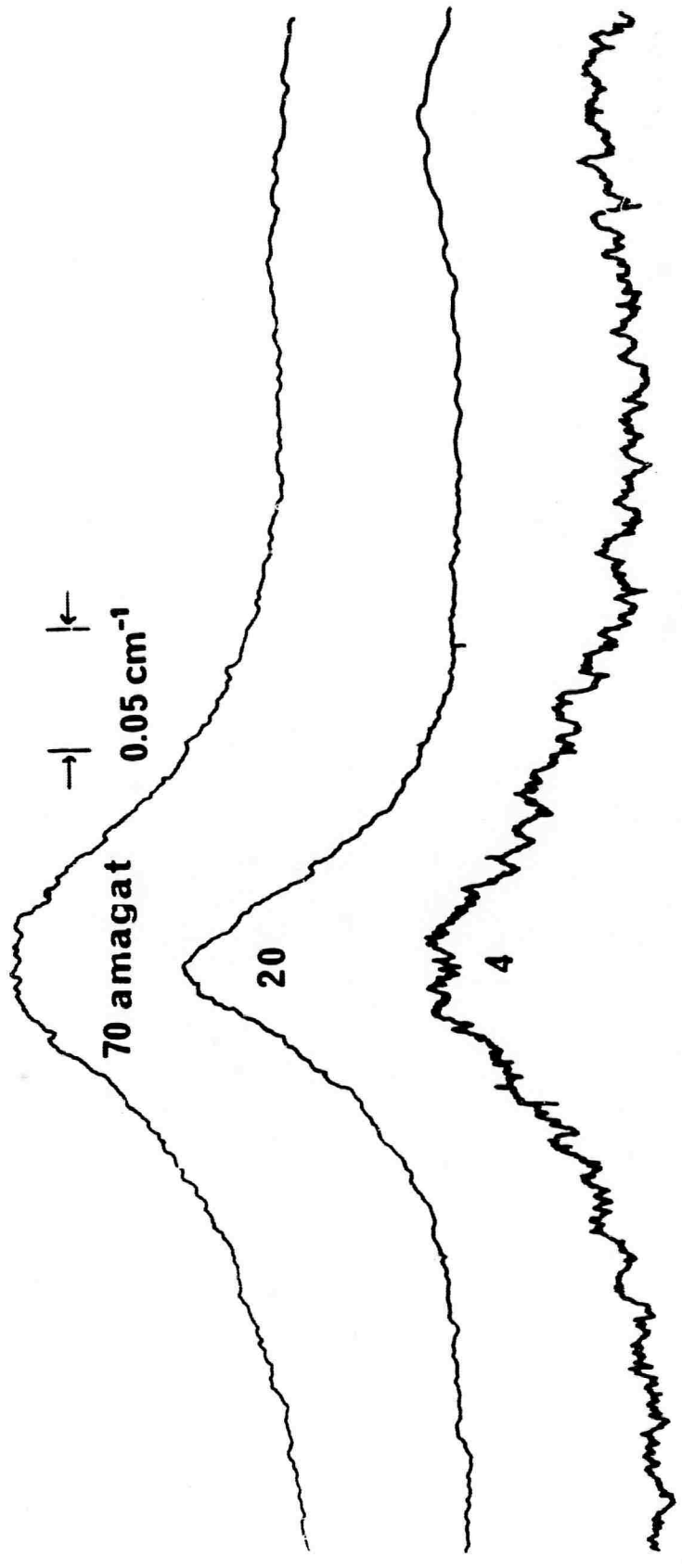
FIGURE CAPTIONS

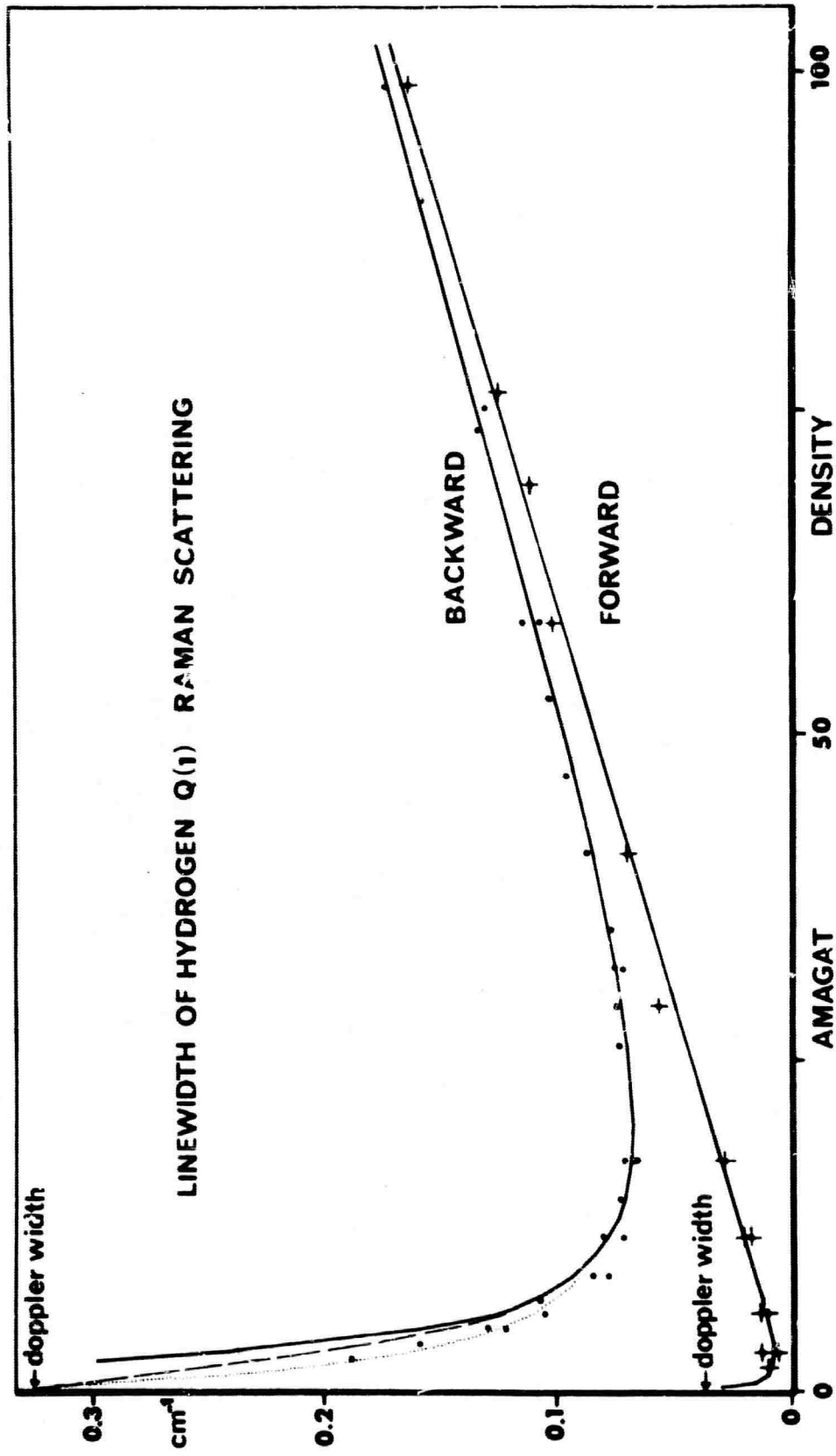
Fig. 1: Sample chart recordings of the Q(1) Raman line of hydrogen, showing the dependence of linewidth on pressure. The small peak to the right is the Q(0) line in another order of the interferometer. The scanning speed was $0.025 \text{ cm}^{-1}/\text{min}$ and the time constant 10 sec.

Fig. 2: Linewidth (full width at half maximum) of the Q(1) Raman line of hydrogen for forward and backward scattering. The Doppler broadening is destroyed as the density increases, and pressure broadening then becomes dominant. The instrumental linewidth has been subtracted. The theoretical fits are explained in the text.

FOOTNOTES

1. The line shape should be Lorentzian, and fits a Lorentzian to within the error of the experiment, above 12 Amagat in the backward direction and 2.5 Amagat in the forward direction, so that the Lorentzian instrumental width may be simply subtracted. Below 12 Amagat the lineshape should go smoothly from a Lorentzian to a Gaussian at zero density, but our noise at these low densities is too severe to get a detailed line shape. We have used a best Lorentzian fit to extract the linewidth.





Pressure Dependence of the Decay Rate for Imprisoned
4.35 Micron Spontaneous Emission in CO₂

M. A. Kovacs and A. Javan

We report the measured pressure dependence of the trapped spontaneous decay rate of the (00⁰1-00⁰0) 4.35 micron transition in CO₂. The continued reabsorption and subsequent emission made possible by the heavily populated (00⁰0) state leads to the imprisonment or "trapping" of the 4.35 micron resonance radiation and a pressure dependent trapped decay rate. Present theory⁽¹⁾ for such imprisoned decay rates is valid for an isolated two-level transition, but does not apply directly to a vibration-rotation band where absorption varies over the band and rotational relaxation times may be much shorter than the untrapped spontaneous lifetime.

We have observed a trapped spontaneous decay rate which decreases sharply with increasing CO₂ pressure below 0.2 torr; for higher pressures, this rate decreases slightly with increasing CO₂ pressure.

The measurements were made in a room temperature CO₂-argon mixture confined in a 1" I. D. cylindrical cell and excited by a 10.6 micron laser pulse. This pulse produces a non-equilibrium (00⁰1) state population whose return to equilibrium is monitored by observation of the 4.35 micron

spontaneous emission. For additional experimental details, see Ref. 2. Several conditions dictated operating pressures: the total pressure exceeded 4 torr to minimize the decay rate due to diffusion of excitation to the walls. Then CO_2 - CO_2 and CO_2 -argon collisions and spontaneous emission determined the observed decay rate. It is generally known that the collisional decay of the 00^0_1 excitation occurs in several steps: the first, (step #1), is decay to a nearby vibrational state, (e.g. 03^1_0), followed by decay of this state to many other levels, (step #2). A second restriction limited argon and CO_2 partial pressures to the region where step #1 occurred more slowly than step #2. Then the 00^0_1 state decays as a single exponential whose rate is determined by the step #1. Finally, the operating pressure remained below 10 torr where the 4.35 micron collisional width 4.35 is smaller than the Doppler width. This insures the the trapped decay rate will depend on CO_2 pressure only. The resulting single exponential decay of the 00^0_1 state has decay rate $\gamma = \gamma_{\text{CO}_2-\text{CO}_2} + \gamma_{\text{CO}_2\text{-buffer}} + \gamma_{\text{trapped}}$ where $\gamma_{\text{CO}_2-\text{CO}_2}$, $\gamma_{\text{CO}_2\text{-buffer}}$ and γ_{trapped} are the decay rates for CO_2 and argon volume quenching and the trapped spontaneous decay rate, respectively. By varying the buffer gas and holding the CO_2 pressure fixed, one obtains a straight line curve of observed decay rates vs. argon pressure whose extrapolation to zero buffer gas pressure gives $\gamma_{\text{CO}_2-\text{CO}_2} + \gamma_{\text{trapped}}$. Since $\gamma_{\text{CO}_2-\text{CO}_2}$ ⁽³⁾ is known, one readily finds γ_{trapped} for the given CO_2 pressure. CO_2 pressure ranged from 0.05 torr to 1 torr and the argon pressure, from 4 - 10 torr in 0.5 torr steps. We obtained the data for trapped decay

rate vs. CO₂ pressure given in Fig. 1.

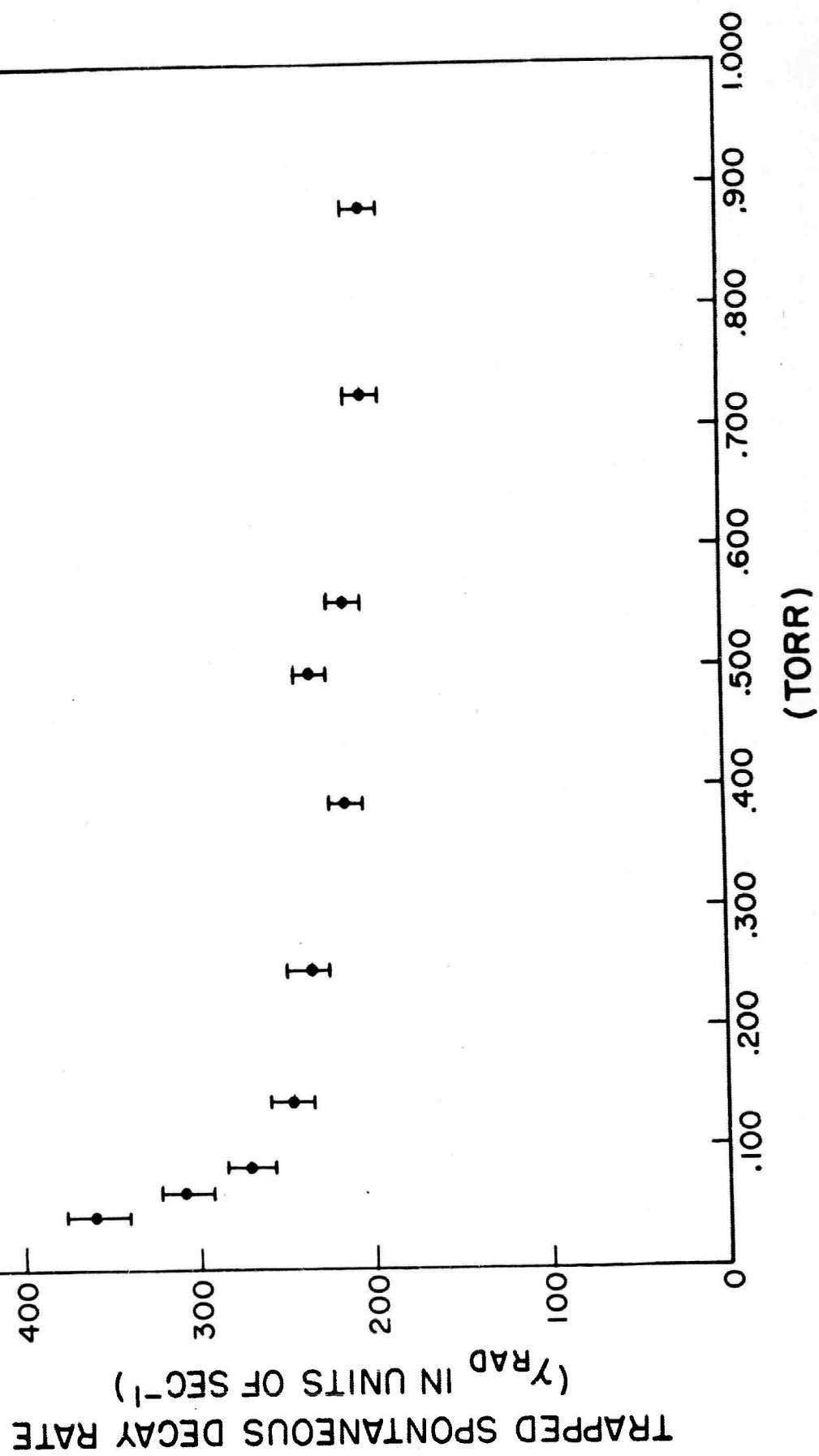
The behavior of the trapped decay rate differs substantially from a $\frac{1}{P[\ln \sigma p]^{1/2}}$ dependence predicted for an isolated Doppler broadened two-level system. The presence of rotational thermalization is significant in the CO₂ case. Since the radiation trapping is sensitive to the lower state population, reabsorption differs for each transition terminating in a different rotational state. Through rotational relaxation, energy transfers from rotational levels at the center of the Boltzmann distribution, where trapping is strong, to levels on the wings, where it is weak. With increasing CO₂ pressure, photons should escape at increasingly high J-states. Preliminary theoretical calculations based on these assumptions are in agreement with the general features of Fig. 1. Details will be published elsewhere.

REFERENCES

1. T. Holstein, Phys. Rev. 72, 1212 (1942).
2. M. A. Kovacs, D. Ramachandra Rao and A. Javan, J. of Chem. Phys. 48, 3339 (1968).
3. C. B. Moore, R. E. Wood, Bei-Lok Hu, and J. T. Yardley, J. of Chem. Phys. 46, 4222 (1967).

FIGURE CAPTION

Imprisoned decay rate vs. pressure for 4.35 emission from CO₂ contained in 1" I. D. cell and uniformly illuminated by 10.6 μ laser pulse.



DOCUMENT CONTROL DATA - R&D

(Security classification of title, body of abstract and indexing annotation must be entered when the overall report is classified)

1. ORIGINATING ACTIVITY (Corporate author) Massachusetts Institute of Technology Cambridge, Massachusetts 02139		2a. REPORT SECURITY CLASSIFICATION Unclassified	
		2b. GROUP	
3. REPORT TITLE "Application of Gas Lasers to Studies of Fundamental Molecular and Atomic Processes"			
4. DESCRIPTIVE NOTES (Type of report and inclusive dates) Annual Technical Report #1 1/1/68 through 12/31/68			
5. AUTHOR(S) (Last name, first name, initial) Professor Ali Javan; Principal Investigator			
6. REPORT DATE January 20, 1969		7a. TOTAL NO. OF PAGES 28	7b. NO. OF REFS 23
8a. CONTRACT OR GRANT NO. N00014-67-A-0204-0014		8b. ORIGINATOR'S REPORT NUMBER(S) Annual Technical Report #1	
b. PROJECT NO. NR 015-717/5-7-68 Code 421		8c. OTHER REPORT NO(S) (Any other numbers that may be assigned this report)	
c. ARPA Order #306			
10. AVAILABILITY/LIMITATION NOTICES Distribution of this document is unlimited			
11. SUPPLEMENTARY NOTES		12. SPONSORING MILITARY ACTIVITY Office of Naval Research Advanced Research Projects Agency ARPA Order # 306	
13. ABSTRACT Measurements related to important aspects of molecular energy transfer and vibrational relaxation in CO ₂ are continuing. Pressure dependence is determined in detail. Measurements of the motional narrowing of the line profile of the spontaneous vibrational Raman scattering in H ₂ are completed. Propagation of short pulses through a resonantly absorbing medium is studied both theoretical and experimentally. In this connection, transmission behavior of 10.6 μ CO ₂ laser radiation pulse is examined in gaseous SF ₆ at varying pressures and new pulse reshaping features are observed in SF ₆ and explained theoretically.			

14. KEY WORDS	LINK A		LINK B		LINK C	
	ROLE	WT	ROLE	WT	ROLE	WT
Molecular relaxation						
Short pulse propagation						
Raman effect						
Self-induced transparency						

INSTRUCTIONS

1. **ORIGINATING ACTIVITY:** Enter the name and address of the contractor, subcontractor, grantee, Department of Defense activity or other organization (*corporate author*) issuing the report.
- 2a. **REPORT SECURITY CLASSIFICATION:** Enter the overall security classification of the report. Indicate whether "Restricted Data" is included. Marking is to be in accordance with appropriate security regulations.
- 2b. **GROUP:** Automatic downgrading is specified in DoD Directive 5200.10 and Armed Forces Industrial Manual. Enter the group number. Also, when applicable, show that optional markings have been used for Group 3 and Group 4 as authorized.
3. **REPORT TITLE:** Enter the complete report title in all capital letters. Titles in all cases should be unclassified. If a meaningful title cannot be selected without classification, show title classification in all capitals in parenthesis immediately following the title.
4. **DESCRIPTIVE NOTES:** If appropriate, enter the type of report, e.g., interim, progress, summary, annual, or final. Give the inclusive dates when a specific reporting period is covered.
5. **AUTHOR(S):** Enter the name(s) of author(s) as shown on or in the report. Enter last name, first name, middle initial. If military, show rank and branch of service. The name of the principal author is an absolute minimum requirement.
6. **REPORT DATE:** Enter the date of the report as day, month, year; or month, year. If more than one date appears on the report, use date of publication.
- 7a. **TOTAL NUMBER OF PAGES:** The total page count should follow normal pagination procedures, i.e., enter the number of pages containing information.
- 7b. **NUMBER OF REFERENCES:** Enter the total number of references cited in the report.
- 8a. **CONTRACT OR GRANT NUMBER:** If appropriate, enter the applicable number of the contract or grant under which the report was written.
- 8b, 8c, & 8d. **PROJECT NUMBER:** Enter the appropriate military department identification, such as project number, subproject number, system numbers, task number, etc.
- 9a. **ORIGINATOR'S REPORT NUMBER(S):** Enter the official report number by which the document will be identified and controlled by the originating activity. This number must be unique to this report.
- 9b. **OTHER REPORT NUMBER(S):** If the report has been assigned any other report numbers (*either by the originator or by the sponsor*), also enter this number(s).
10. **AVAILABILITY/LIMITATION NOTICES:** Enter any limitations on further dissemination of the report, other than those

imposed by security classification, using standard statements such as:

- (1) "Qualified requesters may obtain copies of this report from DDC."
- (2) "Foreign announcement and dissemination of this report by DDC is not authorized."
- (3) "U. S. Government agencies may obtain copies of this report directly from DDC. Other qualified DDC users shall request through _____."
- (4) "U. S. military agencies may obtain copies of this report directly from DDC. Other qualified users shall request through _____."
- (5) "All distribution of this report is controlled. Qualified DDC users shall request through _____."

If the report has been furnished to the Office of Technical Services, Department of Commerce, for sale to the public, indicate this fact and enter the price, if known.

11. **SUPPLEMENTARY NOTES:** Use for additional explanatory notes.
12. **SPONSORING MILITARY ACTIVITY:** Enter the name of the departmental project office or laboratory sponsoring (*paying for*) the research and development. Include address.
13. **ABSTRACT:** Enter an abstract giving a brief and factual summary of the document indicative of the report, even though it may also appear elsewhere in the body of the technical report. If additional space is required, a continuation sheet shall be attached.

It is highly desirable that the abstract of classified reports be unclassified. Each paragraph of the abstract shall end with an indication of the military security classification of the information in the paragraph, represented as (TS), (S), (C), or (U).

There is no limitation on the length of the abstract. However, the suggested length is from 150 to 225 words.

14. **KEY WORDS:** Key words are technically meaningful terms or short phrases that characterize a report and may be used as index entries for cataloging the report. Key words must be selected so that no security classification is required. Identifiers, such as equipment model designation, trade name, military project code name, geographic location, may be used as key words but will be followed by an indication of technical context. The assignment of links, rules, and weights is optional.